Polymer 49 (2008) 2531–2541

Contents lists available at ScienceDirect

Polymer

journal homepage: www.elsevier.com/locate/polymer

Preparation and characterization of microencapsulated polythiol

Yan Chao Yuan [a], Min Zhi Rong [b], Ming Qiu Zhang [b,*]

[a] Key Laboratory for Polymeric Composite and Functional Materials of Ministry of Education, OFCM Institute, School of Chemistry and Chemical Engineering, Zhongshan University, Guangzhou 510275, PR China
[b] Materials Science Institute, Zhongshan University, Guangzhou 510275, PR China

ARTICLE INFO

Article history:
Received 7 December 2007
Received in revised form 13 March 2008
Accepted 28 March 2008
Available online 3 April 2008

Keywords:
Microencapsulation
Synthesis
Polythiol

ABSTRACT

Microcapsules containing curing agent for epoxy were successfully prepared by in situ polymerization with poly(melamine–formaldehyde) (PMF) as the shell material and high-activity polythiol (pentaerythritol tetrakis (3-mercaptopropionate), PETMP) as the core substance. Having been encapsulated, the core material PETMP had the same activity as its raw version. The synthesis approach was so improved that the consumption of polythiol was reduced to a low level. By carefully analyzing the influencing factors including catalyst concentration, reaction time, reaction temperature, feeding weight ratio of core/shell monomers, dispersion rate and emulsifier content, the optimum synthetic conditions were found out. The results indicated that not only core content and size of the microcapsules but also thickness and strength of the shell wall can be readily adjusted by the proposed technical route. The relatively thin shell wall (~0.2 μm) assured sufficient core content even if the microcapsules were very small (1–10 μm). The polythiol-loaded microcapsules proved to be qualified for acting as the mate of epoxy in making two-part microencapsulated healing agent of self-healing composites.

1. Introduction

In recent years, self-healing of thermosetting polymer (mostly epoxy) based composites has attracted increasing attention because they represent an important class of structural materials that require long-term durability and reliability [1–10]. For healing agent aided self-mending, the agent should be liquid at least at the healing temperature. It is generally encapsulated by fragile-walled containers and embedded into the composites' matrix. As soon as the cracks destroy the containers, the healing agent would be released into the crack planes due to capillary effect and bind the cracks as a result of polymerization of the released healing agent.

Dry et al. filled glass pipette tubes with two-part epoxy adhesives consisting of epoxy and amine hardener, respectively, and embedded them into epoxy matrix [1,2]. To eliminate the possibility that the thick hollow glass capillaries might act as initiation for composites failure, Bleay et al. employed hollow glass fibers possessing nearly the same diameter as the reinforcements and applied epoxy-hardener pair as the repair agent [3]. However, filling of repair species into such fine tubes is very difficult. Jung et al. used polyoxymethyleneurea (PMU)-walled microspheres to store an epoxide monomer to be released into cracks and rebond the cracked faces in a polyester matrix [4]. Solidification of the epoxy resin (i.e. the repair action) was triggered by the excessive amine in the composites. White et al. indicated that the method was not feasible as the amine groups did not retain sufficient activity [5].

Zako and Takano proposed an intelligent material system using 40% volume fraction unmodified epoxy particles to repair microcracks and delamination damage in a glass/epoxy composite laminate [6]. By heating to 120 °C, the embedded epoxy particles (~50 μm) would melt, flow to the crack faces and repair the damage with the help of the excessive amine in the composite. Our group also reported a self-healing epoxy composite containing epoxy-loaded poly(urea–formaldehyde) (PUF) microcapsules [7]. The complex of $CuBr_2$ and 2-methylimidazole ($CuBr_2$(2-MeIm)$_4$) served as latent hardener and was pre-dissolved in the matrix during composites' manufacturing. Self-healing of cracks can be conducted at 130 °C as a result of the curing of the released epoxy initiated by $CuBr_2$(2-MeIm)$_4$.

By analyzing the available approaches, it is known that self-healing based on microencapsulated healing agents offers tremendous potential for practical applications [8–10]. This is particularly true when mass production, long shelf life and self-healing free of manual intervention are concerned. However, microencapsulation of hardener for epoxy healing agent is difficult, despite that microcapsules containing epoxy resin are easy to be synthesized by in situ polymerization, complex coacervation and interfacial copolymerization [7,11–14]. The conventional amine-type hardeners for curing epoxy at room temperature are amphoteric and highly active, and hence hard to be encapsulated in water or solvent by

* Corresponding author.
E-mail address: ceszmq@mail.sysu.edu.cn (M.Q. Zhang).

0032-3861/$ – see front matter © 2008 Elsevier Ltd. All rights reserved.
doi:10.1016/j.polymer.2008.03.044

chemical methods. For example, they cannot be encapsulated by PUF under acidic condition. Although physical extrusion art was used to produce some hardener-loaded capsules [15,16], such as the capsules containing mixture of diethylenetriamine and nonyl phenol with alginate wall and the capsules containing diethylamine with thermoplastic wall, they were not suitable for fabricating self-healing composites. The shell wall of the former capsules might suffer from bacterial degradation, while that of the latter was too thick ($\sim$100 μm) to be sensitive to propagating cracks. Moreover, special equipments had to be involved.

Besides amine, polythiols can also used for curing epoxy. Epoxy resin with polythiol as the hardener and strong base as the hardening accelerator is well known for its low-temperature fast curability [17]. Accordingly, microencapsulated epoxy and polythiol might constitute a group of self-healing agent that is able to take effect at or below room temperature. In this context, self-healing can be done free of manual intervention (i.e. heating). To the authors' knowledge, however, microencapsulation of polythiol has not yet been reported. In fact, it is also very difficult to microencapsulate polythiol by the existing techniques like in situ polymerization of urea–formaldehyde or interface polymerization due to the very high activity of hydrosulfide group of polythiol. Liquid polythiol can be cured by a wide variety of compounds including aldehyde, ketone, peroxides, epoxy resins, isocyanates, acrylic and anhydrides through a number of reaction paths such as oxidation, addition and substitution reactions of hydrosulfide terminal groups [18–25]. In most cases, hollow spheres with very thick wall rather than the desired capsules have to be obtained.

To solve the problem, the authors of the present work planed to try another method via in situ polymerization of melamine–formaldehyde in an oil-in-water emulsion. Compared to urea–formaldehyde, polymerization of melamine–formaldehyde proceeds faster and poly(melamine–formaldehyde) (PMF)-walled microcapsules are superior to PUF-walled microcapsules in mechanical properties, stability and chemical resistance [26–29]. In this context, there is a possibility that the consumption of polythiol might be substantially reduced. In situ polymerization with PMF or methanol etherified PMF has been applied to encapsulate liquids such as dye solution [26], dicyclopentadiene [27], lauryl alcohol [30], fragrant oil [31,32] and methylparathion [33]. To obtain microcapsules with sufficient strength, the encapsulation process was usually conducted at higher pH value of 3.5–6.5 and higher temperature of 60–80 °C or longer reaction time of 3–8 h. Although these rigorous processing parameters had little effect on the aforesaid inert core materials, they may lead to failure of microencapsulation or excessive consumption of the active core material, e.g., polythiol in the present work. Therefore, it is necessary to explore suitable reaction conditions (like catalyst concentration, reaction time and temperature, feeding weight ratio of core/shell monomers, dispersion rate and emulsifier content) and illuminate the mechanism of in situ polymerization for microencapsulation of polythiol. It is hoped that our method would greatly reduce consumption of polythiol during encapsulation and help to control the thickness and strength of shell wall.

In this paper, the feasibility of the proposed approach and structure and properties of the resultant microcapsules were examined, so as to provide preparation parameters for making self-healing composites in the subsequent works.

2. Experimental

2.1. Raw materials

Polythiol (pentaerythritol tetrakis (3-mercaptopropionate), PETMP, boiling point = 275 °C at 1 mm Hg, density = 1.28 g ml^{-1} at 25 °C and hydrosulfide group content = 26.55%) used as the core material to be encapsulated was purchased from Fluka Chemie AG (Buchs, Switzerland). Melamine (M), analytically pure agent, was provided by Shanghai First Chemical Co., China. Formaldehyde (F), analytically pure agent, 37 wt.%, was supplied by Guangzhou Chemical Co., China. Triethanolamine and citric acid used for controlling pH value of solution were provided by Shanghai Medical Group Reagent Co., China.

Styrene, maleic anhydride, and the initiator dibenzoyl peroxide (BPO) were purchased from Shanghai Medical Group Reagent Co., China. Diglycidyl ether of bisphenol A (DGEBA, EPON 828) was supplied by Shell Co. as the composite's matrix resin. Diglycidyl tetrahydro-*o*-phthalate (DTP) was provided by Tianjin Jindong Chemical Plant, China as the polymerizable component of the healing agent. Diethylenetriamine (DETA) was supplied by Shanghai Medical Group Reagent Co., China working for DGEBA. The catalyst benzyl dimethylamine (BDMA) with boiling point 183.5 °C was purchased from Shanghai Medical Group Reagent Co., China.

2.2. Preparation of the emulsifier poly(styrene–maleic sodium) (PSMS) solution

BPO-initiated copolymerization of styrene and maleic anhydride at 1:1 molar ratio was carried out in toluene solution at 75 °C for 3 h. The average molecular weight and molecular weight distribution of poly(styrene–maleic anhydride) were determined by gel permeation chromatography (GPC) measurements on a Waters Breeze relative to polystyrene standards. That is, $M_n = 8.9 \times 10^3$ and $M_w/M_n = 2.3$. According to the results of element analysis, the contents of styrene and maleic anhydride were found to be 50.6 and 49.4 wt.%, respectively. The 10 wt.% neutral hydrolyzed solution was prepared by dissolving the copolymer in sodium hydroxide solution, and stirred at 80 °C for 5 h.

2.3. Preparation of the microcapsules

PETMP was added into an aqueous solution of PSMS (150 ml). The mixture was vigorously dispersed by a homogenizer for 5 min at a selected rate and then two drops of 1-octanol were added to eliminate surface bubbles of the emulsion. The pre-condensate of M (0.04 mol) and F (0.12 mol) was prepared at 70 °C for 30 min and the pH value of the solution was kept at about 9–10 by adding triethanolamine (Fig. 1(a)). Subsequently, the pre-condensate solution was added to the above emulsion with 450 rpm continuous mechanical agitation by a two-bladed stirring paddle while the pH value of the solution was kept at about 2.7–3.5 by adding citric acid. Eventually, the reaction mixture was cooled to room temperature. The resultant slurry was neutralized by sodium carbonate solution, and then diluted with deionized water. The deposit of

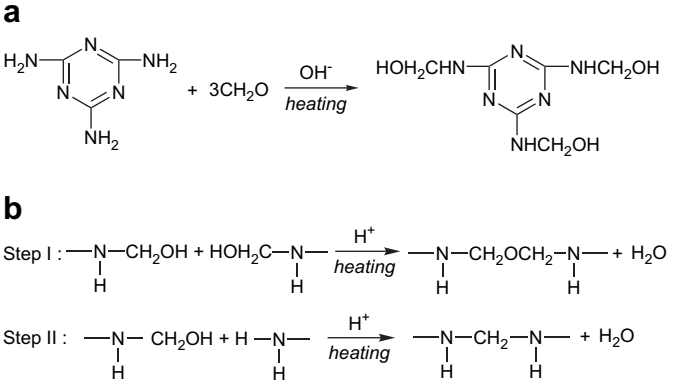

Fig. 1. Reaction schemes of M–F resins. (a) Formation of M–F pre-condensate. (b) Formation of PMF.

Table 1
Descriptions of the microcapsules prepared using different processing parameters

Sample ID	Reaction time (min)	Reaction temperature (°C)	System pH	Feeding weight ratio of core/shell monomers	Emulsifier content (%)	Dispersion rate ($\times 10^3$ rpm)	Average diameter (μm)	Core content (%)	Loss factor (%)	Yield (%)
1-1	20	50	3.2	2.3	2	15	–	–	–	41.5
1-2	40	50	3.2	2.3	2	15	11.5	77.6	10.2	80.7
1-3	60	50	3.2	2.3	2	15	11.5	77.3	10.4	80.8
1-4	80	50	3.2	2.3	2	15	11.5	76.4	11.2	81.0
2-1	60	40	3.2	2.3	2	15	23.2	86.2	3.7	77.9
2-2	60	50	3.2	2.3	2	15	11.3	78.5	10.0	79.8
2-3	60	60	3.2	2.3	2	15	9.3	67.1	16.6	86.7
2-4	60	70	3.2	2.3	2	15	16.1	59.0	23.7	90.2
3-1	60	50	2.7	2.3	2	15	12.2	78.8	7.2	82.1
3-2	60	50	2.9	2.3	2	15	12.2	81.7	5.8	80.3
3-3	60	50	3.2	2.3	2	15	11.3	77.6	10.7	80.2
3-4	60	50	3.5	2.3	2	15	11.9	76.9	12.9	79.0
4-1	60	50	3.2	0	2	15	6.0	0	–	36.5
4-2	60	50	3.2	1.2	2	15	9.4	33.1	45.3	88.2
4-3	60	50	3.2	1.7	2	15	8.7	71.8	14.3	83.3
4-4	60	50	3.2	2.3	2	15	11.4	76.9	10.5	81.2
4-5	60	50	3.2	2.9	2	15	13.9	87.4	6.5	79.3
5-1	60	50	3.2	2.3	1	15	36.3	83.5	4.7	79.5
5-2	60	50	3.2	2.3	2	15	11.5	77.6	10.2	80.6
5-3	60	50	3.2	2.3	3	15	5.4	70.8	13.2	85.5
6-1	60	50	3.2	2.3	2	10	36.7	83.8	8.0	76.6
6-2	60	50	3.2	2.3	2	15	11.8	77.6	10.1	80.7
6-3	60	50	3.2	2.3	2	20	5.0	67.7	12.8	91.7

microcapsules was separated through a Buchner funnel and rinsed with deionized water and acetone, and then vacuum dried. Fig. 1(b) shows the condensation reaction scheme of M–F resins. Table 1 lists the influences of the processing parameters on the resultant microcapsules as well as the sample IDs.

A comparison experiment was conducted using PUF to encapsulate PETMP. The preparation processes were the same as those applied for making PMF-walled microcapsules, except that the content of urea was 0.06 mol.

2.4. Preparation of epoxy composite containing the polythiol-loaded microcapsules

The unfilled epoxy specimens were produced through mixing 100 parts EPON 828 epoxy resin with 12 parts curing agent DETA. The filled epoxy composites were prepared by uniformly mixing 10 wt.% of the PETMP-loaded microcapsules together with the aforesaid mixture of EPON 828 and DETA. To obtain cured version, the unfilled epoxy and the filled version were degassed and poured into closed silicone rubber molds and cured for 24 h at room temperature, followed by 24 h at 40 °C.

2.5. Characterization

Fourier-transform infrared (FTIR) spectra were obtained by Bruker EQUINOX 55 FTIR spectrometer to identify the chemical structure of the specimens, which were prepared by grinding the samples with potassium bromide (KBr) or by attaching the samples to a KBr disc.

Average diameter, size distribution and specific surface area of the resultant microcapsules were determined by a Malvern MasterSizer 2000 Particle Size Analyzer.

Surface morphology and shell thickness of the microcapsules were monitored by scanning electron microscopy (FEI/OXFORD/HKL Quanta 400FEG and Philips XL30-FEG). The microcapsules' residue produced by grinding or acetone extraction was mounted on a conductive stage to facilitate membrane thickness measurement prior to observation. The samples were sputtered with a thin layer (~10 nm) of gold–palladium to prevent charging under the electron beam. The appearance of the microcapsules was also observed by optical microscope (Orthoplan Pol, Leitz).

Micro-Raman measurements were carried out using a Renishaw inVia (UK) spectrometer equipped with a Leica microscope system. Raman spectra were excited by a 785 nm laser line at a resolution of 1 cm^{-1}, and the laser was focused by a 20× objective to a spot size of about 1 μm. These parameters were kept constant for all the samples. The spectra were calibrated using the 520.0 cm^{-1} line of a silicon wafer.

Thermogravimetric analyses (TGA) of the microcapsules were carried out using Netzsch TG-209. The samples were heated from 25 to 600 °C at a rate of 10 °C min^{-1} under the protection of nitrogen flow.

Both isothermal and non-isothermal curing kinetics were studied by differential scanning calorimetry (DSC) with a TA DSC Q10 calorimeter under the protection of nitrogen flow. The heating rate for the non-isothermal measurements was 5 °C min^{-1} from −20 to 100 °C. Calibration of the calorimeter with regard to temperature and energy was achieved by measurement of the temperature and enthalpy of melting of indium as standard material.

Storage stability of the microcapsules was characterized by their weight loss exposed to room temperature at periodical intervals and heat treatment at different temperatures, respectively.

Yields of the preparation were defined by the ratio of the mass of the collected microcapsules to the total feeding mass of PETMP core and shell monomers.

2.6. Determination of core content and loss factor

The microcapsule's core content and loss factor were determined by elemental analysis and extraction method. Using acetone as extraction solvent, the microcapsule samples were extracted by Soxhlet apparatus for 240 h to remove the core material. The contents of N and S elements of the samples were examined using a carbon-hydrogen-nitrogen-sulfur (CHNS) analyzer (Vario EL, Germany Elementar Inc.). The initial N and S contents of the intact microcapsules are denoted by $W_{N(i)}$ and $W_{S(i)}$, while the N and S contents of the residual shell wall are denoted by $W_{N(r)}$ and $W_{S(r)}$. As N element in either the microcapsule or the residual shell wall should completely come from melamine rings in the microcapsule wall material and its amount remained

unchanged before and after the extraction, the shell wall content (W_{wall}) and core content (W_{core}) can thus be calculated from:

$$W_{wall} = \frac{W_{N(i)}}{W_{N(r)}} \times 100\% \quad (1)$$

$$W_{core} = \left(1 - \frac{W_{N(i)}}{W_{N(r)}}\right) \times 100\% \quad (2)$$

In the course of microencapsulation, some PETMP was consumed form the shell wall. The ratio of the losing part to PETMP in the microcapsules was defined as the loss factor (LF):

$$LF = \frac{W_{S(r)} \times W_{N(i)}}{W_{S(i)} \times W_{N(r)}} \times 100\% \quad (3)$$

3. Results and discussion

3.1. Microencapsulation of polythiol

Formaldehyde mostly presents itself as methylene glycol in formalin and has two active functional groups, while melamine is a weakly basic reagent with six functional groups. Therefore, they can react with each other forming melamine–formaldehyde polymer. In general, the reaction consists of two stages as described in the following (Fig. 1). (i) The nucleophilic addition stage in basic solution proceeds at about 70 °C, when melamine reversibly and successively reacts with formaldehyde to give nine different methylol melamines ranging from mono- to hexamethylol melamines (a typical reaction with trimethylol melamines is shown in Fig. 1(a)). (ii) The condensation stage proceeds in acidic solution at about 50 °C, during which two mechanisms are involved: formation of ether bridges via the reaction between two methylol groups and formation of methylene bridges via the reaction between a methylol group and an amino group with elimination of water (cf. steps I and II in Fig. 1(b)) [34–37]. The condensation stage overlaps in time with the in situ polymerization or the microencapsulation process.

During the in situ polymerization, M–F monomers and the pre-condensate reacted with each other in acidic water phase to form low molecular weight oligomers. These pre-condensate and oligomers possess surface activity like surfactants because their molecular structure contains both hydrophilic and hydrophobic groups [38,39]. Consequently, the M–F pre-condensate and oligomers tended to gather together at the phase boundary between the dispersed water insoluble core substance PETMP droplets and the aqueous volume phase. The driving force for the enrichment at the surface of the dispersed phase was the surfactant character of the M–F pre-condensate and oligomers. The higher concentration of the reactive resin molecules (i.e. the M–F pre-condensate and oligomers) in the boundary layer must favor the condensation reaction. In other words, the resin condensation proceeded much faster at the interface than in the volume phase. As a result, gel-like structures were built up at the beginning owing to liquid–liquid phase separation, which was further hardened to give the capsule walls [39]. Subsequently, integrity and mechanical strength of the capsules' wall were enhanced owing to the increased thickness and cross-linking degree of PMF. These mean that the condensation reaction kinetics of M–F must play a key role in the course of microencapsulation.

In fact, the condensation reaction rate and degree are determined by reaction time, reaction temperature and catalyst H^+ concentration [37]. These factors are investigated in detail herein after trying to find out the optimum conditions. As illustrated by Figs. 2 and 3, the microcapsules prepared at excessively short reaction time (20 min, for example, see Fig. 2(a)), or excessively high pH value (3.5, for example, see Fig. 2(h)), or excessively low reaction temperature (40 °C, for example, see Fig. 3(a)) cannot maintain their integrity after drying because of the weak shell walls, in spite of holding spherical shape in water. When the reaction time exceeds 40 min, microcapsules' shape, yield and loss factor do not show significant change with the reaction (refer to Fig. 2(b)–(d) and the samples 1-2 to 1-4 in Table 1).

Comparatively, the influence of pH value on reaction kinetics is quite complex due to interference of the parallel reactions taking place at the condensation stage. When the pH value of solution is reduced, the yield slightly increases (refer to the samples 3-1 to 3-4 in Table 1). At pH = 2.9, both loss factor and core content reach their minimum and maximum values of 5.8 and 81.7%, respectively. This implies that higher catalyst concentration may accelerate the condensation reaction, so that less time is left for the reaction between the polythiol and M–F pre-condensate and oligomers. Meanwhile, the stronger walls generated at lower pH values facilitate formation of spherical microcapsules, as shown in Fig. 2(e)–(g).

It is worth noting that some hollow microcapsules resulting from air bubbles appear in the case of low pH value (Fig. 2(e) and (f)). The amount of the hollow microcapsules seems to increase

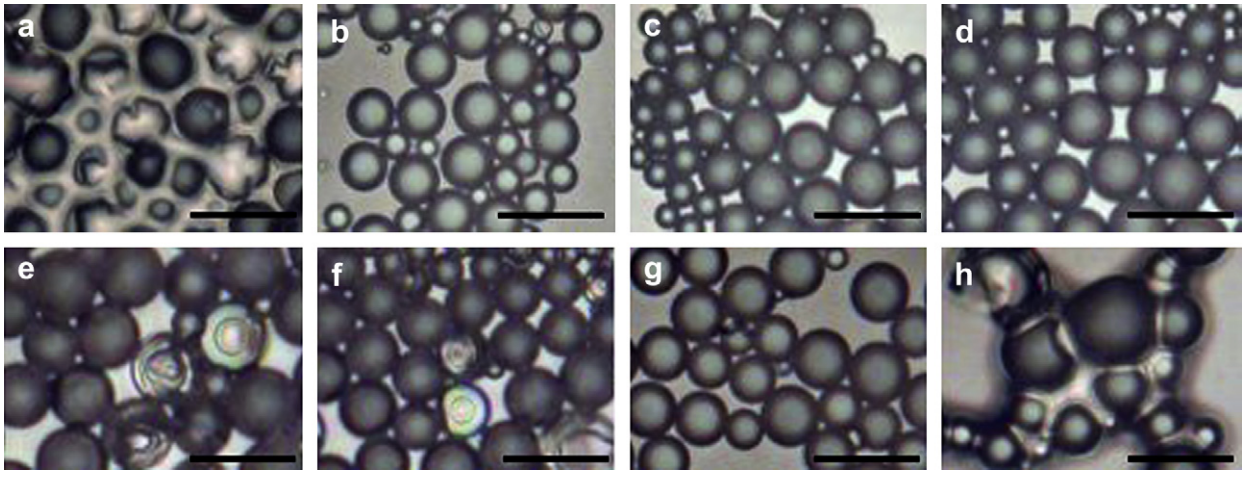

Fig. 2. Optical microscopic images of the PMF-walled microcapsule prepared under different conditions: (a) 20 min, 50 °C, pH = 3.2; (b) 40 min, 50 °C, pH = 3.2; (c) 60 min, 50 °C, pH = 3.2; (d) 80 min, 50 °C, pH = 3.2; (e) pH = 2.7, 60 min, 50 °C; (f) pH = 2.9, 60 min, 50 °C; (g) pH = 3.2, 60 min, 50 °C; (h) pH = 3.5, 60 min, 50 °C. The attached scale bars represent 20 μm in length.

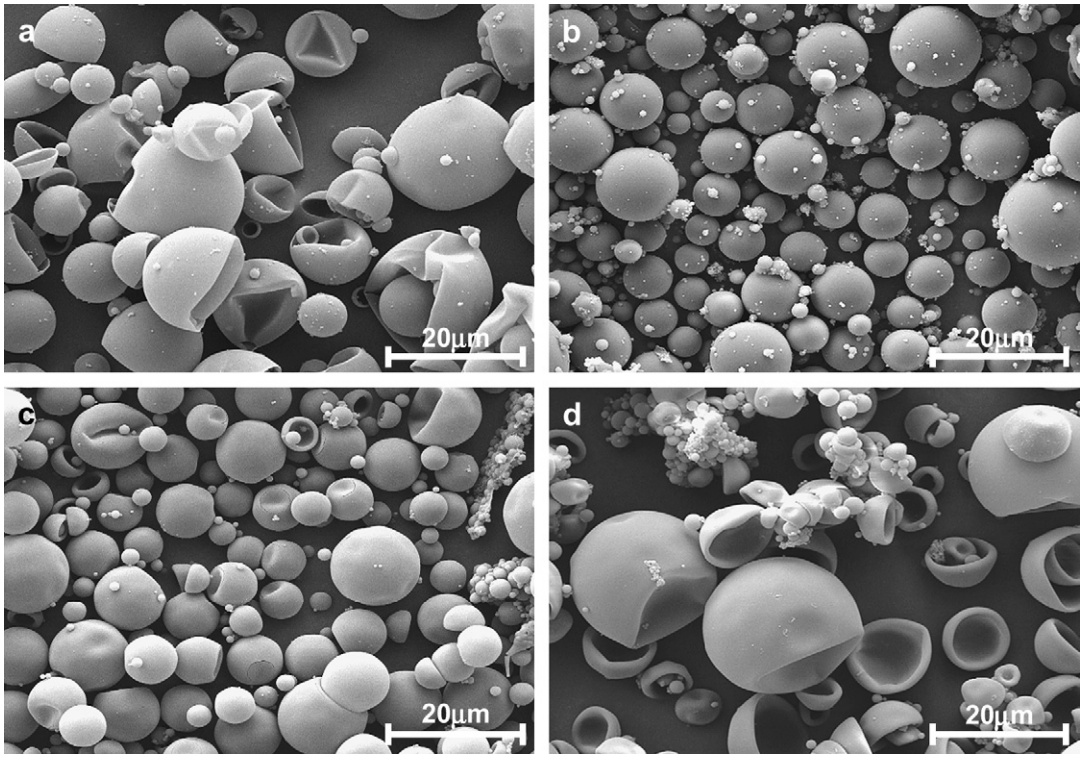

Fig. 3. SEM micrographs of PMF-walled microcapsules prepared at (a) 40 °C, (b) 50 °C, (c) 60 °C, and (d) 70 °C. Conditions of synthesis: 60 min, pH = 3.2.

with decreasing the pH value. It is attributed to the fact that a faster condensation reaction increases the probability of wall formation on the surface of air bubbles. Increased number of hollow microcapsules would consume much wall materials and might reduce the quality of microcapsules containing PETMP. Consequently, an appropriate catalyst concentration (pH = 2.9–3.2) is required to balance the loss factor, core content, as well as the amount of hollow microcapsules.

On the other hand, Fig. 4(a) shows that a few powder-like PMF nanoparticles adhere to the microcapsules. They should be formed by the M–F oligomers through successive polymerization, liquid–liquid phase separation and deposition in the aqueous volume phase along with ceaseless decrease of their solubility [32,40]. Compared with UF microcapsules, the surfaces of the M–F microcapsules are smoother [7,11,41]. In addition, the relative higher yields of M–F microcapsules indicate that the outgrowth of PMF nanoparticles is not significant. Yield of microencapsulation is defined as the ratio of the mass of the collected microcapsules to the total feeding mass of PETMP core and shell monomers. Table 1 shows that the yields of most experiments fall inside the limits of 76–92% except samples 1-1 and 4-1. In fact, the amounts of hollow microcapsules and PMF nanoparticles greatly affect the yield. In the diluted resultant slurry, the microcapsules containing PETMP gradually deposited because their density (1.24 g cm^{-3}) is higher than that of water. However, the hollow microcapsules and some PMF nanoparticles used to be thrown away as they were suspended in the solution.

The emulsifier PSMS adsorbed at the interfaces of the oil droplets is neutral at pH ~3. Its molecules tended to have such directional arrangement with hydrophobic groups oriented into the oil droplet and hydrophilic groups out of the oil droplets, establishing a steric boundary layer around each droplet [38,42,43]. This emulsifier layer allowed the M–F pre-condensate and oligomers to pass through itself and to accumulate at the interface because of their surface activity. When the M–F pre-condensate and oligomers were gradually polymerized and hardened, the newly formed walls began to protect the core materials [38]. Actually, no PSMS molecules can be found on the microcapsules' wall by FTIR and NMR analysis, implying that the external emulsifier has been washed away.

In short, in situ polymerization of melamine–formaldehyde can be successfully used to prepare microcapsules containing polythiol. Under certain conditions, satisfactory microcapsules with high yielding and core content but lower loss factor can be obtained. Surprisingly, the loss factor in most cases is about 10% or even lower. This demonstrates that our idea proposed in Section 1 works, i.e.

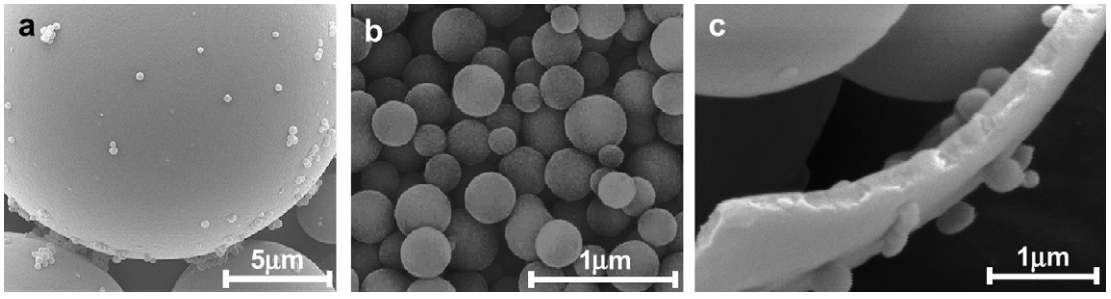

Fig. 4. SEM micrographs of (a) PMF-walled microcapsules, (b) PMF nanoparticles, and (c) broken PMF-walled microcapsules (that had been extracted with acetone) showing the shell wall section. Conditions of synthesis: (a, b) 60 min, 50 °C, pH = 3.2; and (c) 60 min, 60 °C, pH = 3.2.

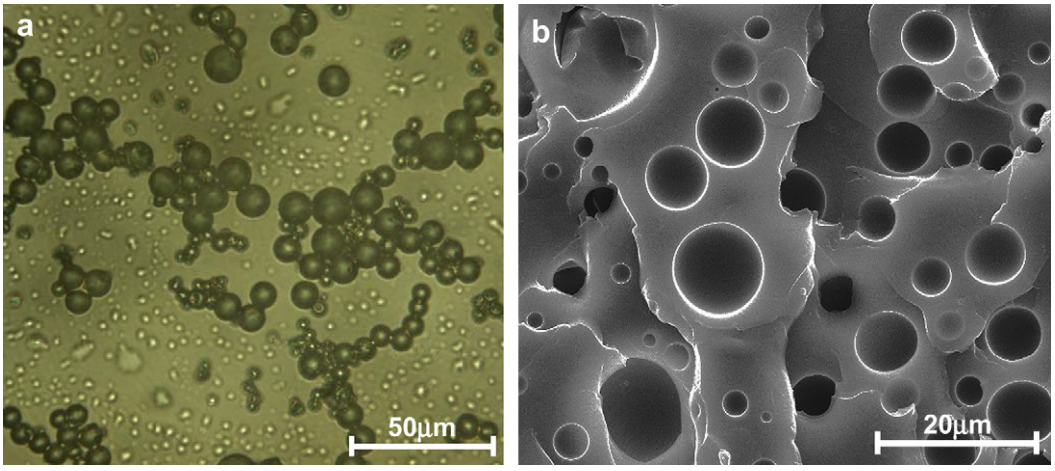

Fig. 5. Optical microscopic and SEM photos of (a) PMF-walled microcapsules dispersed epoxy diluted by acetone and (b) fractured surface of cured epoxy filled with PMF-walled microcapsules, in which the PETMP core was rinsed away by acetone prior to the observation. Conditions of synthesis of the PMF-walled microcapsules: 60 min, 50 °C, pH = 3.2.

a faster condensation reaction between melamine and formaldehyde would help to reduce polythiol consumption. Besides, the polythiol has four –SH groups and acts as a curing agent to form cross-linking network whenever it reacts with M–F pre-condensate and oligomers. Thus, the inner layer of polythiol core is hard to contact the outside M–F pre-condensate and oligomers because the cross-linking film hinders diffusion of the components from both sides.

If PMF were replaced by PUF for the microencapsulation, no intact microcapsules would be obtained because the slower reaction rate led to weak shell. Even though the shell strength of PUF-walled microcapsules can be enhanced by increasing reaction time, and/or reaction temperature and/or catalyst concentration, the core content had to be very low (<20%) and many hollow spheres with very thick wall were produced. Excessive consumption of the active core material and different microencapsulation mechanism of U–F resins should take the responsibility.

3.2. Morphology of the microcapsules and shell thickness

Morphology inspection is important for verifying the resultant of the microencapsulation. Optical microscopic observation of PMF-walled microcapsules showed appearance of diffraction rings. According to the theory of optics, when core and shell in a microcapsule have different refractive indexes, diffraction rings would be perceived at the interface between them [11]. Therefore, it is known that PMF has successfully microencapsulated PETMP with single capsule structure.

To have a general view of the microcapsules, SEM micrographs were taken. Fig. 3(b) indicates that the microcapsules are spherical with diameter of about 10 μm, and their outer surfaces are smooth and compact. Some PMF nanoparticles and their aggregates are attached to the microcapsules' surface. A magnified image of the PMF nanoparticles (i.e. sample 4-1 in Table 1, in which no core material is encapsulated) show that their diameters are about 150–350 nm (Fig. 4(b)), which are nearly independent on the reaction conditions.

The wall thickness can be estimated from Fig. 4(c). That is about 210 nm for sample 2-3. The inner surface of the microcapsule is also smooth and compact. Having examined all the microcapsules, we found that there is nearly no variation in shell wall thickness within the same microcapsule, while the microcapsules prepared under different conditions have slightly different wall thickness (ranging from 150 to 350 nm).

The morphological observation implies that the formation rate and the cross-linking degree of the shell wall must be sufficiently high, and the nanoparticles separated from the aqueous phase didn't react with the wall to yield polynuclear surface structure like the case of PUF-walled microcapsules [7,27,30,41]. In fact, the present microcapsules (~10 μm in diameter) with thin shell wall (~0.2 μm) offer enough interior space for storing the core substance, which guarantees high healing efficiency when the microcapsules serve as self-healing agent.

To assess whether the microcapsules having such shell thickness are robust enough to survive handling during manufacturing self-healing composites, simulative experiments were made. Fig. 5(a) showed that in the mixture with uncured epoxy matrix, the microcapsules are not damaged by the prior processing (i.e. mechanical stirring, ultrasonication and vacuum degasification). Moreover, after curing of the epoxy resin, the embedded microcapsules still maintain their integrity and are well adhered to the matrix (Fig. 5(b)). Evidently, the microcapsules meet the requirement of practical application in terms of their stability with composite fabrication.

3.3. Chemical structure of the microcapsules and activity of the core material

Besides morphological characterization, chemical structure of the resultant microcapsules should be understood (Fig. 6). For PMF,

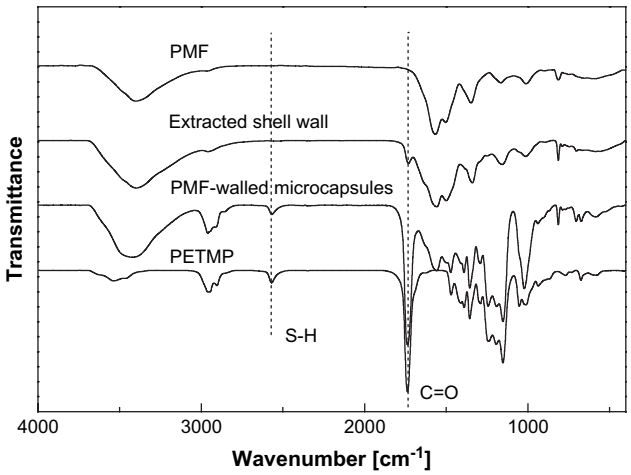

Fig. 6. FTIR spectrum of PMF-walled microcapsules in comparison with those of PMF, extracted shell wall and core material. Conditions of synthesis of the PMF-walled microcapsules: 60 min, 50 °C, pH = 3.2. When the mixture of PMF-walled microcapsules and KBr was ground during sample preparation for FTIR measurement, the microcapsules were broken.

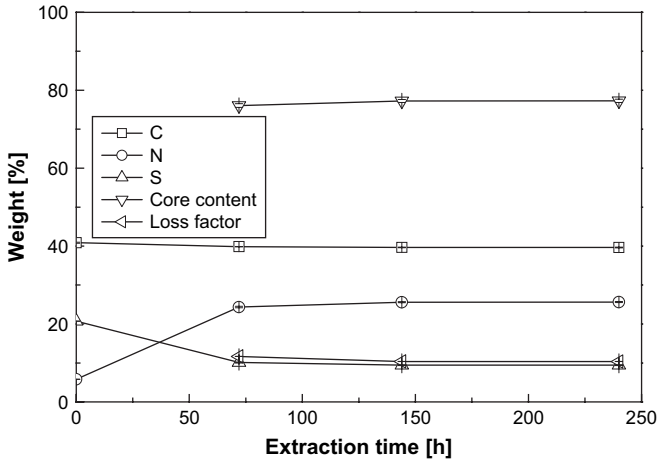

Fig. 7. Effect of acetone extraction time on elements' contents, core content and loss factor of the extraction residue of the ground PMF-walled microcapsules. Conditions of synthesis of the PMF-walled microcapsules: 60 min, 50 °C, pH = 3.2. For ensuring complete extraction, both ground and intact microcapsule samples had been measured, respectively. It was found that the results are hardly different, so that the data in this figure were only collected from the ground microcapsules.

its FTIR spectrum exhibits board stretching vibration of N–H and O–H at 3390 cm^{-1}, stretching of C═N at 1565 cm^{-1} and characteristic stretching peak of triazine ring at 814 cm^{-1}. Meanwhile, the spectrum of PETMP reveals S–H stretching mode at 2568 cm^{-1} and C═O stretching at 1737 cm^{-1}, respectively. Clearly, in the spectrum of the broken microcapsules, all the characteristic peaks of both PMF and PETMP appear, which confirms that PETMP has been encapsulated by PMF.

Owing to the high activity of hydrosulfide group, polythiol is able to react with aldehyde or ketone via addition reaction [18]. M–F pre-condensate or oligomers also possess high activity, and their self-condensation or co-condensation with poly(ols) would easily take place because of the active methylol groups and formaldehyde [34,36]. The reversible addition of thiols to aldehydes and ketones can be conducted with acidic or basic catalyst [19], and polycondensation reaction of bis-thiols with formaldehyde and acetone is allowed to proceed in alkaline medium [44]. Besides, hydrogen sulfide might react with formaldehyde in acid medium to form a hydrosulfide adduct [45]. It means that the core material PETMP might probably react with formaldehyde and/or methylol groups of M–F pre-condensate or oligomers during the microencapsulation.

Fig. 7 shows the dependence of C, N and S contents, core content and loss factor of the ground microcapsules on acetone extraction time. It is seen that within the time range 144–240 h, the elements' contents, core content and loss factor are almost the same, meaning a further increase in the extraction time is unnecessary. Although the core material must have been fully extracted, there is still 9.45 wt.% S element in the residual shell wall of the microcapsules after extraction (Fig. 7). In other words, 10.37 wt.% PETMP was consumed in the course of microencapsulation for constructing the shell wall, and hydrosulfide groups in the consumed PETMP took part in the cross-linking or condensation reaction with M–F pre-condensate or oligomers. This phenomenon was also detected in the microcapsules prepared under other conditions. In fact, FTIR spectra of the related materials are also able to evidence the above analysis from another angle (Fig. 6). By using peak area of carbonyl group as the internal standard for showing fraction of hydrosulfide groups, S–H/C═O peak area ratio of raw PETMP is estimated to be 4.33×10^{-2}, while that of the broken microcapsules is about 2.83×10^{-2}. The reduction in S–H/C═O peak area ratio suggests that hydrosulfide groups of PETMP must have been partly consumed when the microcapsules were produced. Besides, the characteristic stretching peak of C═O rather than S–H appears in the spectrum of residual shell wall of the microcapsules after extraction. It is indicative of deactivated polythiol in the shell wall. These again reflect that the reaction between polythiol and M–F oligomers is restricted due to the formation of cross-linking network.

Since some of the core material PETMP has been involved in the synthesis of the shell wall, it should be known whether the rest portion keeps the chemical activity. Fig. 8 shows the micro-Raman spectra of a raw PETMP droplet on cured epoxy resin substrate and the PETMP flowing out from the broken PMF-walled microcapsules embedded in cured epoxy. The stretching peak of S–H appears at 2573 cm^{-1} and that of C═O at 1738 cm^{-1}, which conform to the characteristic adsorptions in the FTIR spectra (Fig. 6). When peak area of carbonyl group serves as the internal standard, the S–H/C═O peak area ratio of raw PETMP and the core material from the broken microcapsules are estimated to be 1.72 and 1.62, respectively. The values are very close, demonstrating that PETMP remains unchanged after being encapsulated. On the other hand, the accompanying microphoto of Fig. 8 suggests that the microcapsules embedded in the epoxy matrix are able to rupture and release their core material at the damaged sites, which meets the needs of self-healing composites.

The reactivity of the core material can be further evaluated by DSC measurement (Fig. 9). The heating DSC scans indicate that with a rise in temperature no reaction occurs in either the mixture of

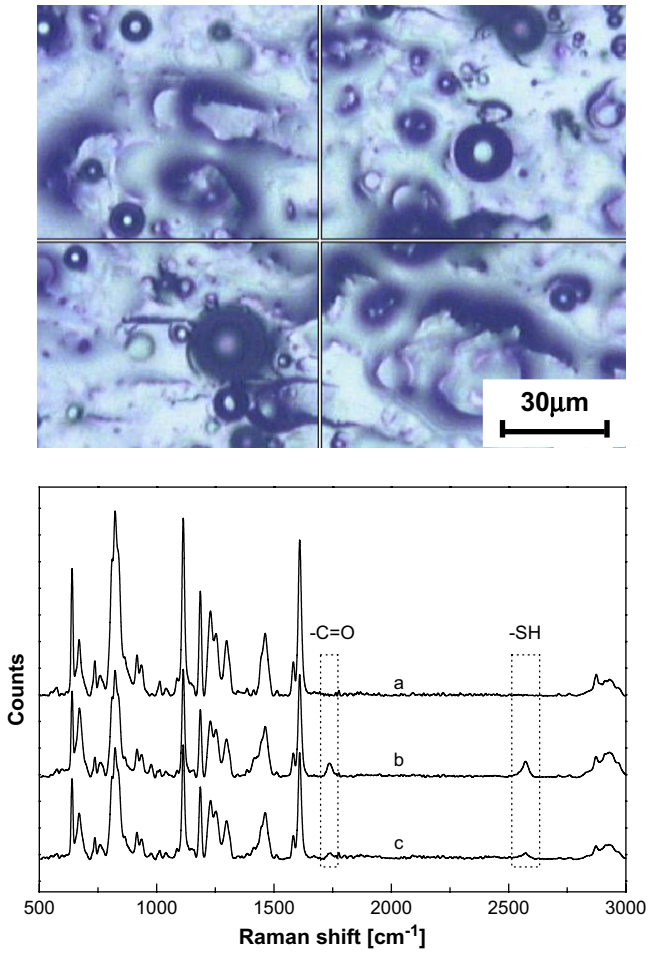

Fig. 8. Micro-Raman spectra of (a) cured epoxy; (b) a raw PETMP droplet on cured epoxy resin substrate and (c) the PETMP flowing out from the broken PMF-walled microcapsules embedded in cured epoxy. The accompanying microphoto shows the fractured surface of cured epoxy filled with PMF-walled microcapsules. The center of the cross indicates the position where the spectrum (c) was collected.

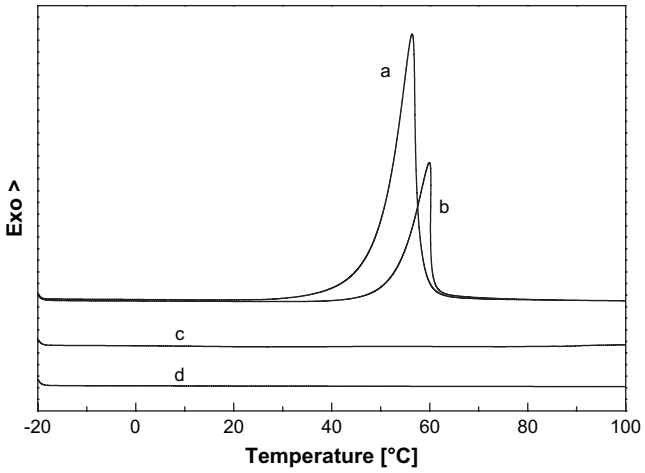

Fig. 9. DSC heating traces of (a) epoxy (DTP)/PETMP/BDMA = 10.9/8.7/1, (b) epoxy (DTP)/ground PMF-walled microcapsules/BDMA = 10.9/19.2/1, (c) epoxy (DTP)/BDMA = 10.9/1, and (d) epoxy (DTP)/PETMP = 10.9/8.7. The compositions are expressed in terms of weight ratios.

epoxy (DTP) and the catalyst BDMA or the mixture of epoxy (DTP) and PETMP. For the mixture of epoxy (DTP)/PETMP/BDMA, however, an obvious exothermic reaction is detected. The peak temperature is 56.4 °C and the heat of reaction is 466.3 J/g. When PETMP was replaced by the ground microcapsules containing PETMP, similar exothermic peak with a heat of reaction of 212.6 J/g appears at 59.9 °C. The difference might result from the fact that (i) grinding of the microcapsules cannot ensure 100% breakage and the quantity of the released core material failed to reach the stoichiometric ratio of DTP to PETMP; and (ii) both shell wall and intact microcapsules were inert and do not take part in the curing reaction.

3.4. Core content and loss factor of the microcapsules

In the course of microencapsulation of PETMP, as discussed in the last section, some PETMP was consumed to build up the shell wall. Considering that excessive reduction in the core content would lower the repair efficiency of the future self-healing composites, loss factor of the encapsulated material and core content should be studied. It is worth noting that although all the processing parameters exert more or less influence on the core content and loss factor, the effects of reaction temperature and feeding weight ratio of core to shell monomers seem to be much more significant.

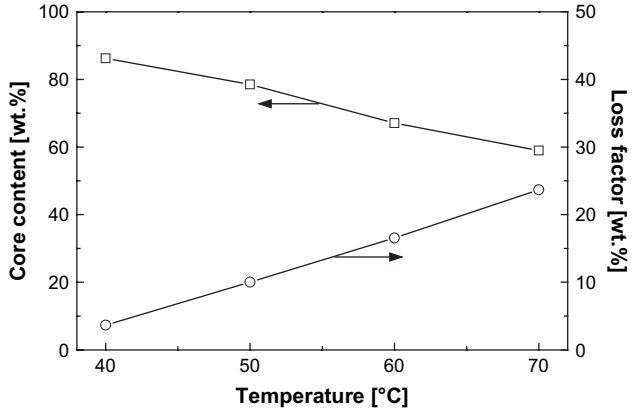

Fig. 10. Effect of reaction temperature on core content and loss factor of PMF-walled microcapsules. Conditions of synthesis of the PMF-walled microcapsules: 60 min, pH = 3.2.

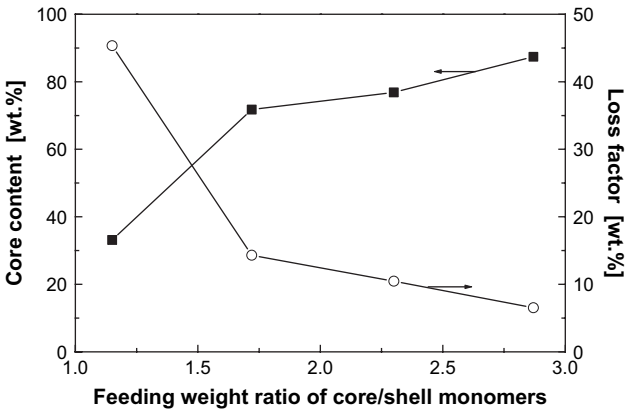

Fig. 11. Effect of feeding weight ratio of core/shell monomers on core content and loss factor of PMF-walled microcapsules. Conditions of synthesis: 60 min, 50 °C, pH = 3.2.

As illustrated in Fig. 10, with increasing reaction temperature, the core content decreases while the loss factor increases. Accordingly, morphologies of the microcapsules prepared at different temperatures are different (Fig. 3). Moreover, the amount of PMF nanoparticles also increases and their aggregation extent is gradually enhanced with temperature. A careful survey of the micrographs in Fig. 3 indicates that except for the microcapsules prepared at 50 °C (Fig. 3(b)), the rest microcapsules have collapsed and shrunk to different extents. Because the reaction rate slows down at lower reaction temperature (40 °C, for instance), the shell wall of the microcapsules has to be thinner, the cross-linking degree of the shell wall material becomes lower, and the deposition quantity of PMF nanoparticles is reduced. Consequently, the core content of the microcapsules is higher and the loss factor is smaller. The weak shell wall would easily cause collapse and shrinkage of the capsules. On the other hand, as higher reaction temperature (60 or 70 °C, for instance) accelerates the reaction, the shell wall of the microcapsules would be thicker, coupled with higher cross-linking degree and larger deposition quantity of PMF nanoparticles. Eventually, the core content is lower and the loss factor is higher. Fig. 3(c) and (d) shows that some of the microcapsules prepared under the very conditions also fail to keep their integrity, probably because (i) substantial core material was consumed to induce shrinkage of the microcapsules and (ii) more drastic collision among the microcapsules in the lower-viscosity solution at elevated temperature leads to collapse of the capsules.

To view the problem from another angle, the effect of feeding weight ratio of core/shell monomers is exhibited in Figs. 11 and 12. As the feeding weight ratio of core/shell monomers increases, the core content increases and loss factor decreases. The amount of PMF nanoparticles and their aggregation extent also decrease. In particular, when the feeding weight ratio of core/shell monomers is 1.2, the core content reaches the lowest value while loss factor the highest. About half of the core material was consumed during microencapsulation as overmuch M–F pre-condensate or oligomers have reacted with PETMP. In the case of feeding weight ratio of core/shell monomers of 2.9, although the core content becomes the highest and loss factor the lowest, the weak shell wall has to result in a great number of collapsed and shrunk microcapsules.

Besides reaction temperature and feeding weight ratio of core/shell monomers, dispersion rate and emulsifier content also influence the core content and loss factor by changing microcapsules' diameter and specific surface area, which will be discussed in the next section. The smaller capsules with larger specific surface area certainly impart a higher loss factor. The pH value of solution is another parameter that should not be neglected as it controls the

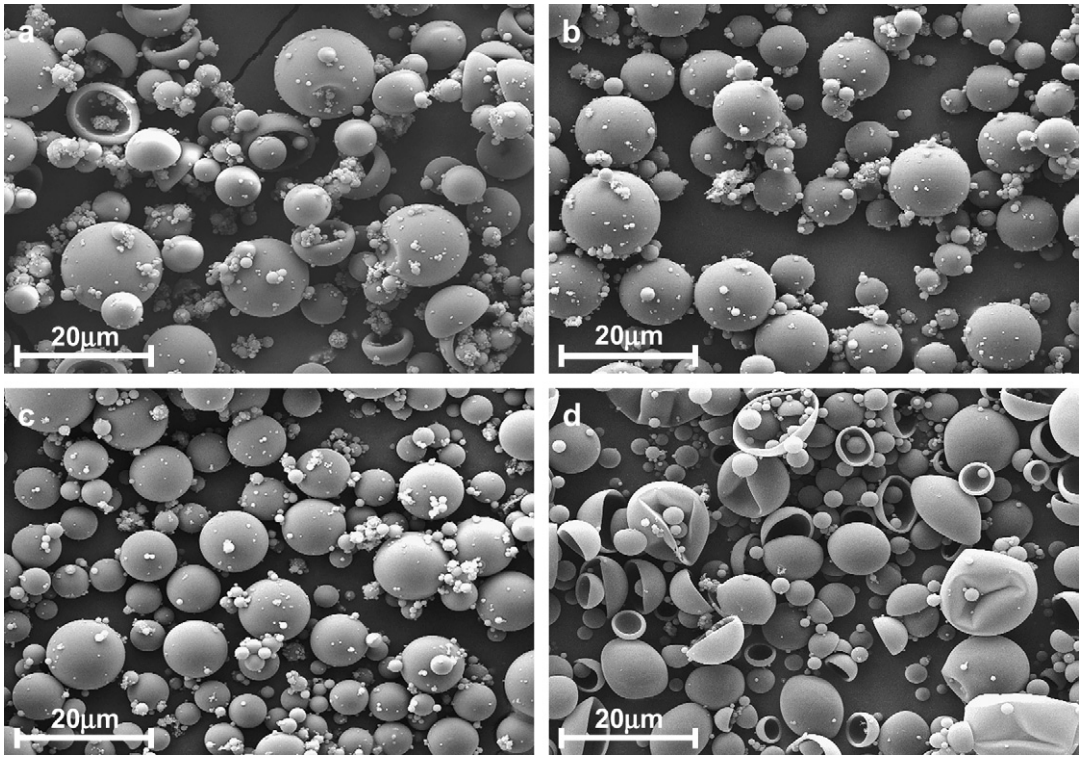

Fig. 12. SEM micrographs of PMF-walled microcapsules with different feeding weight ratios of core/shell monomers: (a) 1.2, (b) 1.7, (c) 2.3, and (d) 2.9. Conditions of synthesis: 60 min, 50 °C, pH = 3.2.

reaction rate of M–F pre-condensate or oligomers. The faster the condensation reaction, the lower the loss factor.

3.5. Size and size distribution of the microcapsules

Before being encapsulated, PETMP had to experience emulsification. Since the shell wall thickness of the microcapsules varies within the narrow limits of 150–350 nm, the size and size distribution of the microcapsules have to be mainly determined by the geometry of the core material droplets formed in the emulsification stage. In this context, dispersion rate of the homogenizer for making the emulsion is critical, and emulsifier content is also important for keeping the body of PETMP droplets in shape.

Fig. 13 shows that higher dispersion rate yields finer emulsion. As a result, with increasing the dispersion rate, the microcapsules average diameter decreases and their size distribution becomes narrow. It is worth noting that there is a small shoulder peak at about 1 μm on each size distribution curve (Fig. 13). It might represent the aggregates of PMF nanoparticles. The inset of Fig. 13 gives the plots of average diameter and specific surface area of the microcapsules against dispersion rate on log–log scale. Linear relationships are observed, which coincides with the results of other researchers (e.g., PUF-walled microcapsules containing diluted epoxy [11], PMF-walled microcapsules containing dicyclopentadiene [27] and PUF-walled microcapsules containing dicyclopentadiene [41]). The influence of emulsifier content is shown in Fig. 14. When the emulsifier content is increased, a finer emulsion is obtained. Accordingly, the microcapsule's average diameter decreases and their size distribution is narrowed down.

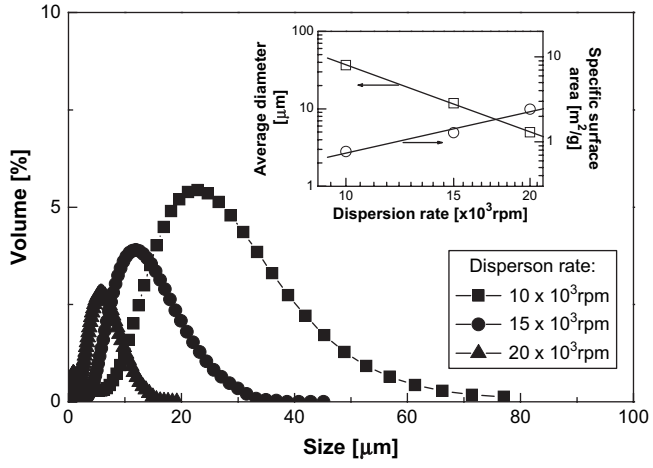

Fig. 13. Effect of dispersion rate on size distribution of PMF-walled microcapsules at a constant emulsifier content of 2%. Conditions of synthesis: 60 min, 50 °C, pH = 3.2.

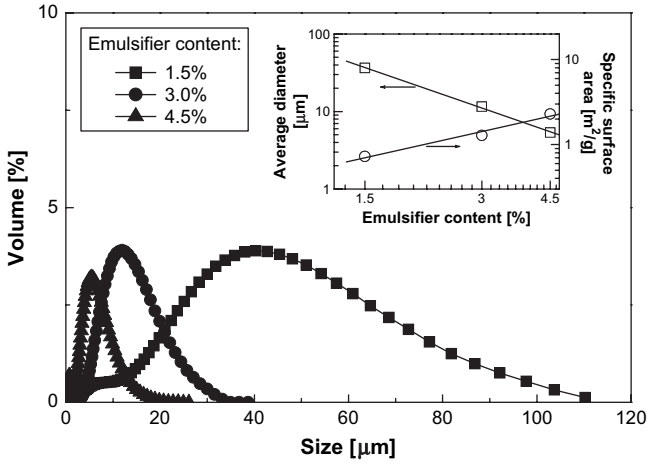

Fig. 14. Effect of emulsifier content on size distribution of PMF-walled microcapsules at a constant dispersion rate of 15×10^3 rpm. Conditions of synthesis: 60 min, 50 °C, pH = 3.2.

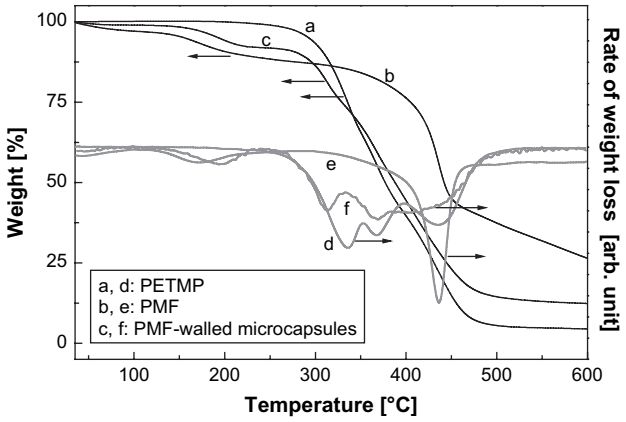

Fig. 15. TG and DTG curves of PMF-walled microcapsules in comparison to those of the shell wall and core material. Conditions of synthesis of the PMF-walled microcapsules: 60 min, 50 °C, pH = 3.2.

3.6. Stability of the microcapsules

When self-healing composites are thermally cured, the embedded microcapsules have to experience heat impact. Therefore, their thermal stability should be known first. From the pyrolytic behaviors shown in Fig. 15, it is seen that there are three main phases of weight loss for the shell wall PMF within the temperature range of interests. The first phase with ~2% weight loss from 25 to 100 °C should be due to evaporation of the adsorbed water. The second phase with ~10% weight loss in the range of 100–270 °C is attributed to evaporation of formaldehyde from the deformaldehyde reaction of PMF at elevated temperature [46]. The third one with ~61% weight loss in the range of 270–600 °C originates from decomposition of a portion of melamine and thermal degradation of PMF [47].

In contrast to PMF, PETMP is quite stable below 250 °C. It also exhibits three stages of pyrolysis from 250 to 600 °C corresponding to its evaporation and decomposition processes. The detailed mechanisms involved need further investigation. Nevertheless, thermal degradation of the PMF-walled microcapsules containing PETMP is a combination of the contributions made by PMF and PETMP. Fig. 15 indicates that the peak pyrolytic temperatures of the microcapsules are not exactly the same as those of the individual components. Thermally induced reaction might occur between the shell and core materials during decomposition.

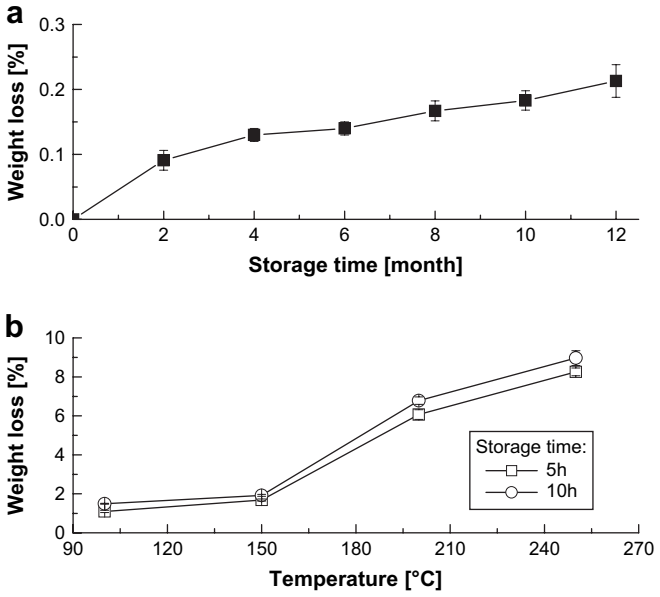

Fig. 16. Effects of storage time and temperature on stability of PMF-walled microcapsules: (a) weight loss of the microcapsules as a function of time at room temperature, and (b) weight loss of the microcapsules as a function of temperatures at constant storage times.

In addition to thermal stability, the microcapsules in service should have long-term stability. Fig. 16 shows effects of storage time and temperature on weight loss of the microcapsules. Evidently, weight loss of the microcapsules exposed to room temperature for six months is only about 0.14 wt.%. When the time is increased to one year, the microcapsules' weight loss is still low (i.e. 0.31 wt.%). Visual inspection does not find any leakage from the microcapsules and their appearance also remains unchanged after long time storage. As the microcapsules were kept in a desiccator and the saturated vapor pressure of polythiol is very low ($\sim 6.5 \times 10^{-11}$ Torr at 25 °C) [48], it can be deduced that the above weight loss should result from evaporation of the physically adsorbed water.

When the storage temperature is increased, weight loss of the microcapsules becomes more and more significant. Staying at higher temperature for longer time would lead to substantial weight loss. It suggests that the microcapsules couldn't be timelessly exposed to heat. At elevated temperature, evaporation of adsorbed water, release of formaldehyde, diffusion of the core material out of shell wall and volatilization of some core material would happen [49,50]. Compared to the microcapsules using PUF as the wall material, the current PMF-walled microcapsules have obviously higher storage stability and heat resistance because of the difference in their chemical structures [50].

4. Conclusions

Microcapsules containing highly active polythiol were successfully prepared by in situ polymerization of melamine–formaldehyde in an oil-in-water emulsion. Surface activity of M–F pre-condensate and oligomers, faster reaction rate, and suitable reaction conditions were found to be the key factors. The mechanism of the microcapsules' formation followed the enrichment and fast curing of M–F oligomers at the surface of polythiol droplets, which ensured lower loss factor.

The synthesis method was improved by optimizing the processing parameters. The appropriate reaction time was about 40–60 min. Further extension of time had little influence on the products. The reaction should proceed at about 50 °C, otherwise the microcapsules might collapse and shrink. The pH value of about 2.9–3.2 was appropriate, which had complex effect on the properties of the products. The feeding weight ratio of core/shell monomers should be set at about 2.3. Size and size distribution of the microcapsules were mainly determined by dispersion rate and emulsifier content. When the microencapsulation was carried out under the suitable conditions mentioned above, loss of core material was greatly reduced, while thickness and strength of shell wall were balanced. Although a small part of the core material PETMP was inevitably consumed for constructing the shell wall, the majority remained unchanged, possessing the same activity as the raw version.

The resultant microcapsules' shell wall was relatively thin (~0.2 μm), which assured sufficient core content even if the microcapsules were very small (1–10 μm). The microcapsules proved to be strong enough to survive handling during manufacturing self-healing composites. Having been pre-embedded in cured epoxy, the microcapsules had satisfied affinity to the matrix, and can be readily ruptured releasing PETMP fluid as expected upon damaging of the composite.

The PETMP-loaded microcapsules had high stability. They can be kept at room temperature for long time and could bear the

moderate temperature or high temperature applied for curing composites.

The present work provided a new approach for producing microcapsules containing hardener for epoxy, which can be used to manufacture self-healing composites or other self-curing stuffs like single constituent epoxy adhesive, self-locking threaded fasteners, etc.

Acknowledgements

The authors are grateful to the support of the Natural Science Foundation of China (Grants: 50573093, U0634001).

References

[1] Dry C, Sottos NR. In: Varadian K, editor. Smart structures and structures 1993: smart materials. Proceedings of SPIE, vol. 1916; 1993. p. 438.
[2] Dry C. Compos Struct 1996;35:263.
[3] Bleay SM, Loader CB, Hawyes VJ, Humberstone L, Curtis PT. Compos Part A 2001;32:1767.
[4] Jung D, Hegeman A, Sottos NR, Geubelle PH, White SR. Compos Funct Grad Mater 1997;80:265.
[5] White SR, Sottos NR, Geubelle PH, Moore JS, Seriram SR, Kessler MR, Brown EN. U.S. Patent 6,858,659 B2; 2005.
[6] Zako M, Takano N. J Intell Mater Syst Struct 1999;10:836.
[7] Yin T, Rong MZ, Zhang MQ, Yang GC. Compos Sci Technol 2007;67:201.
[8] White SR, Sottos NR, Geubelle PH, Moore JS, Kessler MR, Sriram SR, et al. Nature 2001;409(6822):794.
[9] Sottos NR, White SR, Bond I. J R Soc Interface 2007;4:347.
[10] Rule JD, Sottos NR, White SR. Polymer 2007;48:3520.
[11] Yuan L, Liang GZ, Xie JQ, Li L, Guo J. Polymer 2006;47:5338.
[12] Satosdhi M, Ikuzo U, Makoto K, Kunihiko N. E.U. Patent 0,543,675; 1993.
[13] Ronald LH, Dale EW, Colin ED. U.S. Patent 4,536,524; 1985.
[14] Xiao DS, Rong MZ, Zhang MQ. Polymer 2007;48:4765.
[15] Schuetze CE, Antonio S. U.S. Patent 3,396,117; 1968.
[16] Gold Smith CR. U.S. Patent 3,791,980; 1974.
[17] Petrie EM. Epoxy adhesive formulations. New York: McGraw-Hill Co.; 2006 [chapter 5].
[18] Xing QY, Xu RQ, Zhou Z. Fundamental organic chemistry. Beijing: Higher Education Press; 1994 [chapter 25].
[19] Jencks WP, Gilbert HF. Pure Appl Chem 1977;49:1021.
[20] Lowe GB. Int J Adhesion Adhesives 1997;17:345.
[21] Tanaka M, Fujita R, Nishide H. Polymer 2007;48:5884.
[22] Carioscia JA, Stansbury JW, Bowman CN. Polymer 2007;48:1526.
[23] Xu HJ, Chen KC, Guo XX, Fang JH, Yin J. Polymer 2007;48:5556.
[24] Strounina EV, Kane-Maguire LAP, Wallace GG. Polymer 2007;47:8088.
[25] Knauss DM, Edson JB. Polymer 2006;47:3996.
[26] Fuchigami M. U.S. Patent 4,233,178; 1980.
[27] Yuan L, Liang GZ, Xie JQ, He SB. Colloid Polym Sci 2007;285:781.
[28] Sun G, Zhang Z. Int J Pharm 2002;242:307.
[29] Fery A, Weinkamer R. Polymer 2007;48:7221.
[30] Su JF, Li R, Wang LX. Colloid Polym Sci 2005;284:224.
[31] Hong K, Park S. Mater Chem Phys 1999;58:128.
[32] Lee HY, Lee SJ, Cheong IW, Kim JH. J Microencapsulation 2002;19:559.
[33] Dietrich K, Bonatz E, Geistlinger H, Herma H, Nastke R, Purz HJ, et al. Acta Polym 1989;40:325.
[34] Baucer DR. Prog Org Coat 1986;14:193.
[35] Kumar A, Katiyer V. Macromolecules 1990;23:3729.
[36] Jones FN, Chu GB, Samaraweera U. Prog Org Coat 1994;24:189.
[37] Schldknecht CE, Skeist I. Polymerization processes. New York: John Wiley & Sons; 1977 [chapter 6].
[38] Seitz ME. U.S. Patent 5,204,185; 1993.
[39] Dietrich K, Bonatz E, Nastke R, Herma H, Walter M, Teige W. Acta Polym 1990; 41:91.
[40] Jahromi S, Litvinov V, Gelade E. J Polym Sci Part B 1999;37:3307.
[41] Brown EN, Kessler MR, Sottos NR, White SR. J Microencapsulation 2003; 20(6):719.
[42] Braun D, Sauerwein R, Hellmann GP. Macromol Symp 2001;163:59.
[43] Garnier G, Duskova-Smrckova M, Vyhnalkova R, Van de Ven TGM, Revol JF. Langmuir 2000;16:3757.
[44] Angiolini LG, Carlini C, Tramontini M, Ghedini N. Polymer 1990;31:353.
[45] Shanthi K, Balasubramanlan N. Microchem J 1996;53:168.
[46] Costa L, Gamino G. J Therm Anal 1988;34:423.
[47] Devallencourt C, Saiter JM, Fafet A, Ubrich E. Thermochim Acta 1995;259:143.
[48] http://www.brunobock.org/.
[49] Zhang XX, Tao XM, Yick KL, Wang XC. Colloid Polym Sci 2002;282:330.
[50] Yuan L, Liang GZ, Xie JQ, Guo J, Li L. Polym Degrad Stab 2006;91:2300.